

Constraining Age of Deformation Stages in the South-Western Part of Verkhoyansk Fold-and-Thrust Belt by Apatite and Zircon Fission-Track Analysis

S. V. Malyshev^{a, b, *}, A. K. Khudoley^a, U. A. Glasmacher^c, G. G. Kazakova^d, and M. A. Kalinin^d

^a*Institute of Earth Sciences, St. Petersburg State University, St. Petersburg, 199034 Russia*

^b*Institute of Precambrian Geology and Geochronology, Russian Academy of Sciences, St. Petersburg, 199034 Russia*

^c*Institute of Earth Sciences, Heidelberg University, Heidelberg, 69120 Germany*

^d*Karpinsky Russian Geological Research Institute, St. Petersburg, 199106 Russia*

**e-mail: s.malyshev@spbu.ru*

Received January 28, 2018

Abstract—Zircon fission track analysis was carried out for Mesoproterozoic to Lower Paleozoic sedimentary rocks of the South-Verkhoyansk sector of the Verkhoyansk fold-and-thrust belt. The age of thrusting stages was constrained in this region. The early stage of deformations dated as 160 Ma, the main stage dated as from 70 to 90 Ma. Thermal history modeling on apatite allowed us to establish the youngest stage of erosion from 20 to 30 Ma, which indirectly indicates the reactivation of tectonic processes in the region at the boundary of Paleogene and Neogene. The degree of heating of the rocks increases in the east direction, and if in the frontal zone the fission tracks were annealed only in apatite, then in the Sette-Daban zone fission tracks were annealed both in apatite and in zircon.

Keywords: Riphean, Paleozoic, fission-track analysis, thermal modelling, deformations stages, South-Verkhoyansk sector, Kyllakh and Sette-Daban zones

DOI: 10.1134/S0016852118060055

INTRODUCTION

The South Verkhoyansk sector is included in the Verkhoyansk fold-and-thrust belt and is located in its southern part (Fig. 1). The sector extends roughly from north to south along the Aldan River, separated from the Siberian Platform by a range of frontal thrusts. This sector consists of three tectonic zones characterized by different deformations and rocks of various age [8]. The Verkhoyansk fold-and-thrust belt formed under great coeval Late Mesozoic tectonic events such as the collision of the Siberian paleocontinent with the Kolyma–Omolon terrane located east of it and accretion processes along the Okhotsk active continental margin [3, 8, 11]. The age of deformations is constrained by the following data.

(1) The fold-and-thrust structure of the Siberian southeastern margin is cut by granites with a crystallization age of 92–123 Ma obtained by ⁴⁰Ar/³⁹Ar dating [34].

(2) The Priverkhoyansk foredeep formed in the frontal zone of the Verkhoyansk fold-and-thrust belt in the Late Jurassic–Early Cretaceous [6, 32, 38]; it was filled with clastic material removed from the Siberian Platform [2, 16].

(3) Single apatite fission track dates in the Kyllakh zone that evidence erosion of the thrust sheets 70–80 Ma [1, 9, 40].

These data make it possible to approximately estimate the age of the deformation stages. For a more detailed analysis of thrust and deformation processes, we used: apatite (AFT) and zircon fission tracks (ZFT) dating. This method helps to date the cooling stages of minerals commonly related to areas of uplift and erosion and determine the erosion rate. In addition, using of differences in the closure temperatures of apatite and zircon and the method of thermal modeling allows specifying the burial depths and thermal history of the sedimentary complexes.

Terrigenous complexes containing apatite and zircon are abundant in the Verkhoyansk fold-and-thrust belt. The formation processes of the fold-and-thrust structures, well-defined on maps on a scale of 1 : 1000000 or larger [13], resulted in large uplifts and their subsequent erosion, recorded by the track systems.

The investigation objective is to establish:

(1) age of deformations in the South Verkhoyansk sector;

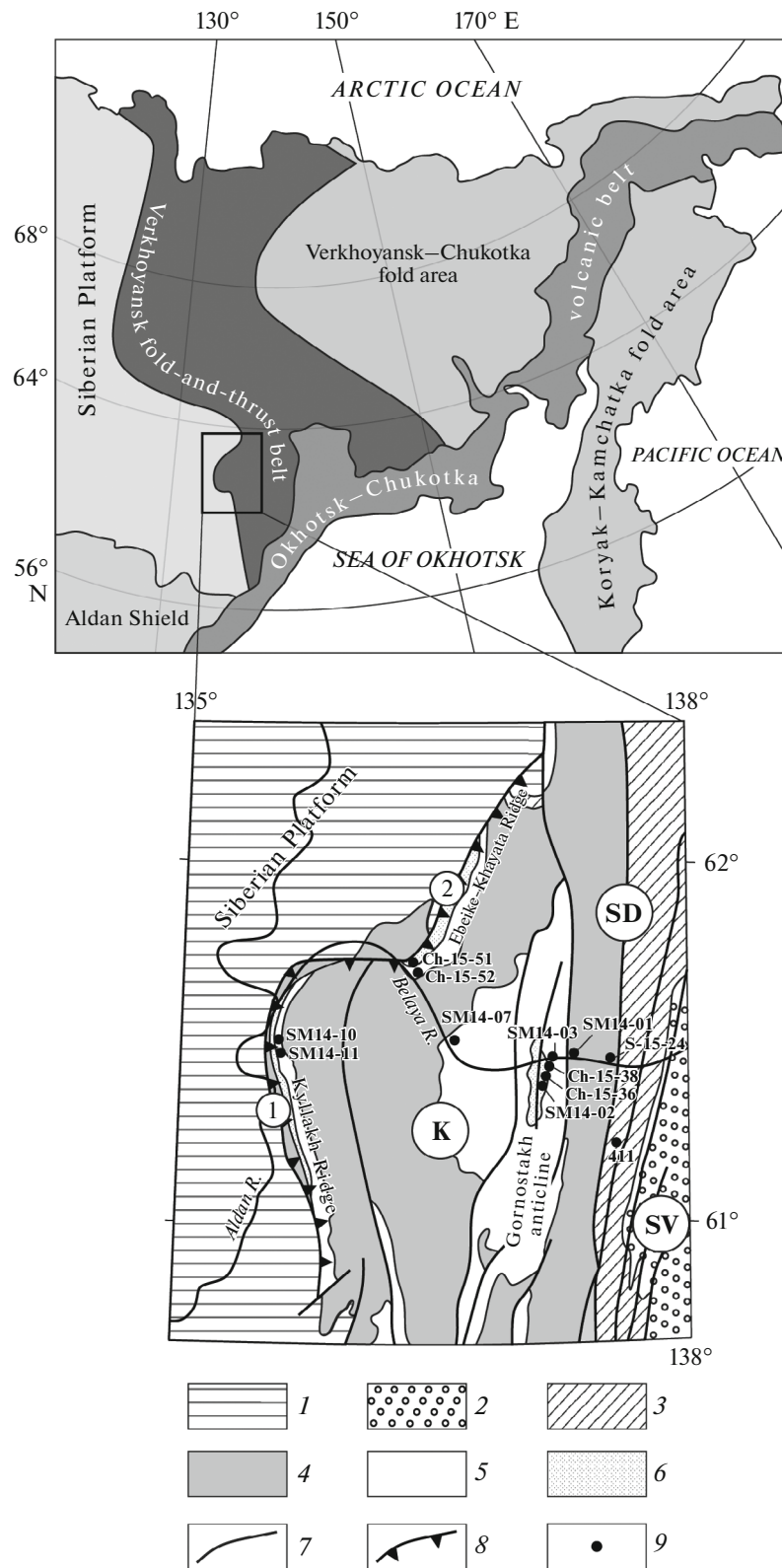


Fig. 1. Geological map of study area and its position on tectonic map of Northeast Asia (using data of [8, 10, 11, 13]). Tectonic zones: (K) Kyllakh, (SD) Sette-Daban, (SV) South Verkhoyansk. Numerals mark frontal thrusts on the margin of Siberian Platform: (1) Kyllakh, (2) Ebeike-Khayata. (1) Jurassic and Cretaceous; (2) Carboniferous and Permian; (3) Ordovician–Silurian–Devonian; (4) Vendian and Cambrian; (5) Middle and Upper Riphean; (6) Lower Riphean; (7) overthrusts; (8) marginal suture of Siberian Platform; (9) sampling points.

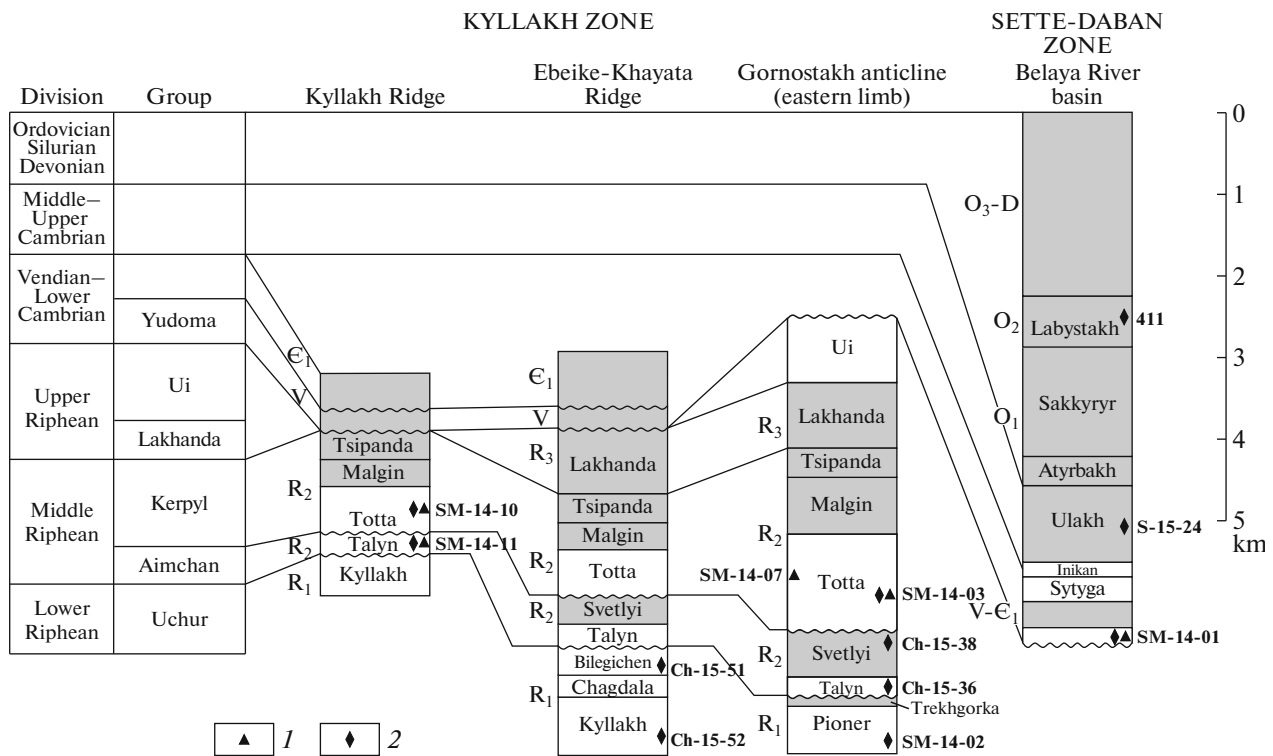


Fig. 2. Position of studied samples in composite stratigraphic sections of Kyllakh and Sette-Daban zones in South Verkhoyansk region (using data of [7, 10, 13, 15] as amended). Names of formations and groups (columns). Formations composed mainly of rocks: carbonate (gray), terrigenous (white). (1, 2) Fission track analysis in (1) apatite (AFT); (2) zircon (ZFT).

(2) burial depth and amplitude of erosion of rocks in different parts of the South Verkhoyansk sector;

(3) variations in thickness and structure of the Paleozoic sedimentary basin in the transition zone from the shelf of the Siberian paleocontinent to its slope according to the erosion rate data.

GEOLOGY

The South Verkhoyansk sector consists of three tectonic zones: the Kyllakh, Sette-Daban, and South Verkhoyansk [8]. The Kyllakh zone is traced along the margin of the platform and consists of Riphean, Vendian, Cambrian, and Ordovician terrigenous-carbonate sedimentary rocks. The Sette-Daban zone occupies the axial position of the South Verkhoyansk sector and consists mainly of Vendian, Lower, and Middle Paleozoic carbonate deposits. The South Verkhoyansk zone is dominated by Upper Paleozoic-Mesozoic terrigenous rock sequences. The study area is located in the central part of the South Verkhoyansk sector of the Verkhoyansk fold-and-thrust belt and covers the Kyllakh and Sette-Daban zones.

The studied part of the sedimentary section includes Riphean and Lower Paleozoic deposits (Fig. 2). The Lower Riphean sedimentary rocks of the Uchur Group outcrop in the core of the Gornostakh anticline and on the Ebeike-Khayata and Kyllakh ridges. They consist of

multicolored mostly terrigenous and terrigenous-carbonate sediments. The bottom of the Uchur Group is dominated by arkose and oligomictic sandstone, while its top in the Gornostakh anticline is dominated by terrigenous-carbonate cyclites. Analysis of the sedimentary structures has shown that the Uchur Group was deposited in near shore conditions in the intracratonic basin, which deepened eastward and received material from platform areas [5, 30].

Middle Riphean sedimentary rocks, which unconformably overlap Lower Riphean strata, are widespread within the Kyllakh zone (Fig. 2). Clastic rocks predominate in the Talyn Formation at the bottom of the Aimchan Group and in the Totta Formation, marking the beginning of the Kerpyl Formation and a new sedimentation cycle. Other Middle Riphean formations (Svetlyi, Malgin, and Tsipanda) are composed mainly of carbonate rocks. The Talyn Formation consists largely of quartz horizontally and cross-bedded sandstone with well-sorted rounded grains. In the Talyn, the predominant shallow sea settings were replaced by deeper water by the beginning of the deposition of the Svetlyi formation. In the Totta Formation, quartz and subarkose poorly sorted sandstone are replaced upward the section by finer-grained sandstone and shale.

The Upper Riphean deposits begin with the clay-carbonate sequence of the Lakhanda Group. The Upper Riphean sandstones in the study area are

observed only in the overlying Ui Group. Abundant sandstone, immature in the composition of clastic fraction, were deposited under relatively deep-water conditions in a rift setting [10, 30, 31]. The most complete sections of the Ui Group occur in the western limb of the Gornostakh anticline and in the hanging walls of regional overthrusts.

Vendian deposits overlying various Riphean formations with an angular unconformity and deep erosion consist of shallow-marine quartz sandstone, dolomite, and limestone, which form the groundmass of the section. Late Vendian–Early Cambrian rifting in the eastern margin of the Siberian paleocontinent led to the formation of a passive margin [31]. Limestone, marl, and argillite were deposited there in the Cambrian. Further east, shelf sediments are replaced by deep-water slope deposits of the Middle and Upper Cambrian and Lower Ordovician, which are replaced upsection again by shallow carbonate strata of the Middle and Upper Ordovician, Silurian, and Lower Devonian [7, 14].

SAMPLING

Sampling for fission track analysis was carried out from natural outcrops of Riphean, Vendian, and Lower Paleozoic terrigenous rocks in the Belaya River basin along the roughly EW-trending profile, which crosses the Kyllakh and Sette-Daban zones across their strike. Data are given on the location and age for the studied sandstone samples (Table 1; Figs. 1, 2).

The selected sandstone samples cover a stratigraphic interval from the Lower Riphean to the Ordovician. Lower and Middle Riphean strata were sampled in the Kyllakh zone, in the hanging walls of the Kyllakh and Ebeike-Khayata overthrusts, and also within the Gornostakh anticline (Fig. 1). The eastern limb of the anticline is overlain by complexly deformed Vendian–Lower Paleozoic strata of the Sette-Daban zone, from which Vendian, Cambrian, and Ordovician rock samples were taken. In general, zircon tracks were studied in 11 samples; in five samples for apatite tracks (Table 1; Fig. 2).

RESEARCH METHODS

^{238}U fission track dating is used to determine the rock age below the closure temperature of the track system in U-bearing minerals, of which zircon and apatite are the most popular for studying the exhumation history of fold-and-thrust belts [21, 24]. The great importance of these minerals is related to their widespread occurrence in various igneous, metamorphic, and sedimentary rocks, as well as to the high uranium and thorium concentrations. The closure temperature of the track system is estimated at $\sim 110^\circ\text{C}$ for apatite and at $\sim 240 \pm 30^\circ\text{C}$ for zircon [26, 39].

The minerals were dated by the conventional method with using an external detector and ζ -calibra-

tion [25, 28]. Rock crushing and mineral separation for fission track dating were recovered at the Institute of Precambrian Geology and Geochronology, Russian Academy of Sciences (St. Petersburg, Russia); specimen mounting and fission track dating were performed at the Laboratory of Thermochronology and Archaeometry, Heidelberg University (Heidelberg, Germany). The samples were irradiated in the research reactor FRM II (Munich, Germany) in the presence of a glass neutron dosimeter with known uranium content (CN1 and CN5 [18]) together a Durango [36] and a Fish Canyon tuff [37] age standards for apatite and zircon, respectively. All track ages were calculated as central ages [12, 23] with an error of $\pm 1\sigma$. All ages and radial plots were calculated and drawn using computer code TRACKKEY software [20, 22]. The ζ -value of 345 ± 13 for CN5 (apatite) and 123.5 ± 6 for CN1 (zircon) were gained using Durango apatite and Fish Canyon zircon age standards.

In contrast to classical geochronology, when the measured age corresponds to the mineral crystallization age, the apatite fission track system retains information about the mineral cooling process in the temperature range between the complete disappearance and relative stability of the tracks [35]. This temperature range is a partial annealing zone, corresponding to $60\text{--}110^\circ\text{C}$ for apatite [25]. Quantitative estimation of the temperature–time conditions that control fission track annealing in apatite makes it possible to interpret the ages, taking into account the relationship of the decreasing track length and density with the thermal history of a sample [27, 33]. In our study, we performed the estimation by numerical modeling in the HeFTy software [29].

FISSION TRACK DATING DATA

The results of apatite and zircon fission track dating (AFT and ZFT) are given in Tables 2 and 3 and Fig. 3. The apatite track ages occur in a narrow range of 67.5–86.5 Ma, whereas the zircon track ages are in a wide range from 90 to 572 Ma. All obtained age values can be subdivided into four groups:

- (1) ≥ 273 Ma,
- (2) ≈ 162 Ma,
- (3) 115–131 Ma,
- (4) ≤ 92 Ma.

The >273 Ma group includes four samples taken from the Kyllakh and Ebeike-Khayata ridges (Fig. 2, samples SM-14-10, SM-14-11, Ch-15-51, and Ch-15-52). All four samples are characterized by a wide age range of individual grains, reaching 2.5 Ga. Values more ancient than the sedimentary stratum characterize source areas. The age values mostly correspond to the range of 200–800 Ma and thus can be interpreted as partially annealed tracks. In samples SM-14-10 and SM-14-11 from the Kyllakh ridge, the spread of age values in some grains is wider and the

Table 1. Summary data on sandstone samples from South Verkhoyansk sector

Sample	Sample location	N	E	Absolute elevation, m	Rock type	Rock age	Method
<i>Kyllakh Ridge</i>							
SM-14-10	Kyllakh Ridge, Aldan River	61°34'03.6"	135°33'26.3"	180	c/g sandstone	R ₂ tt	AFT ZFT
SM-14-11	Kyllakh Ridge, Aldan River	61°34'30.5"	135°33'17.5"	140	m/g sandstone	R ₂ tl	AFT ZFT
<i>Ebeike-Khayata Ridge</i>							
Ch-15-51	Belaya River, Ebeike-Khayata Ridge	61°43'36.5"	136°23'47.9"	990	c/g sandstone	R ₁ kl	ZFT
Ch-15-52	Belaya River, Ebeike-Khayata Ridge	61°42'8.8"	136°21'45.3"	520	c/g sandstone	R ₂ blg	ZFT
<i>Gornostakh anticline</i>							
SM-14-02	Svetlyi Cr., Gornostakh anticline	61°21'21.9"	137°07'48.3"	710	m/g sandstone	R ₁ pn	ZFT
SM-14-03	Svetlyi Cr., Gornostakh anticline	61°22'03.0"	137°11'20.8"	630	m/g sandstone	R ₂ tt	AFT ZFT
SM-14-07	Belaya River near Gornostyl River mouth	61°27'50.9"	136°58'53.1"	460	f/g sandstone	R ₂ tt	AFT ZFT
Ch-15-36	Svetlyi Cr., Gornostakh anticline	61°21'46.9"	137°09'20.0"	650	m/g sandstone	R ₂ tl	ZFT
Ch-15-38	Svetlyi Cr., Gornostakh anticline	61°22'0.1"	137°10'18.7"	650	f/g sandstone	R ₂ sv	ZFT
<i>Sette-Daban zone</i>							
SM-14-01	Belaya River near Suordakh River mouth	61°22'25.8"	137°19'05.8"	550	c/g sandstone	V jud	AFT ZFT
S-15-24	Belaya River near Setan'ya River mouth	61°24'03.4"	137°43'17.2"	610	Calcareous sandstone	Є ₂ ul	ZFT
411	Rozovyi Cr.–Right Sakhara River	60°56'30.0"	137°34'30.0"	900	Calcareous sandstone	O ₂	ZFT

(AFT) Apatite fission track dating, (ZFT) zircon fission track dating; (f/g) fine-grained, (m/g) medium-grained, (c/g) coarse-grained; (pn) Pioneer Formation, (kl) Kyllakh Formation, (blg) Bilegichen Formation, (tl) Talyn Formation, (sv) Svetlyi Formation, (tt) Totta Formation, (jud) Yudoma Group, (ul) Ulakh Group. Stratigraphic location of samples (Fig. 2).

Table 2. Apatite fission track dates

Sample	Grains, pcs	$\rho_s (N_s)$ ($\times 10^6 \text{ cm}^{-2}$)	$\rho_i (N_i)$ ($\times 10^6 \text{ cm}^{-2}$)	P (χ^2)	Age, Ma $\pm 1\sigma$	Average track length, μm (number of tracks)
<i>Kyllakh Ridge</i>						
SM-14-10	3	5.15 (40)	14.54 (113)	96	86.5 \pm 16.3	—
SM-14-11	12	7.76 (458)	24.45 (1443)	99	77.7 \pm 5.2	13.6 \pm 0.74 (19)
<i>Gornostakh anticline</i>						
SM-14-03	20	5.22 (380)	16.03 (1167)	100	76.4 \pm 5.4	—
SM-14-07	17	2.43 (178)	8.77 (644)	99	67.5 \pm 6.3	13.2 \pm 0.72 (15)
<i>Sette-Daban zone</i>						
SM-14-01	20	3.71 (256)	11.26 (777)	99	80.1 \pm 6.6	13.1 \pm 0.65 (13)

(ρ_s) Spontaneous track density of ^{238}U , (N_s) number of counted spontaneous fission tracks, (ρ_i) induced track density of ^{235}U , (N_i) number of counted induced fission tracks, (P (χ^2)) chi-square probability in percentage.

Table 3. Zircon fission track dates

Sample	Grains, pcs	$\rho_s (N_s)$ ($\times 10^6 \text{ cm}^{-2}$)	$\rho_i (N_i)$ ($\times 10^6 \text{ cm}^{-2}$)	$P(\chi^2)$	Age, Ma $\pm 1\sigma$	U, g/t
<i>Kyllakh Ridge</i>						
SM-14-10	20	230.1(1832)	14.2 (113)	76	424 ± 46	113.60
SM-14-11	10	195.1 (531)	8.8 (24)	94	572 ± 123	65.57
<i>Ebeike-Khayata Ridge</i>						
Ch-15-51	16	189.9 (1037)	18.5 (101)	99	273 ± 31	140.43
Ch-15-52	14	204.1 (825)	18.1 (73)	72	300 ± 40	132.66
<i>Gornostakh anticline</i>						
SM-14-02	20	99.8 (1520)	23.16 (352)	97	115.5 ± 8.9	174.46
SM-14-03	20	101.8 (1370)	20.9 (281)	80	130.8 ± 11.1	169.34
Ch-15-36	20	120.9 (1400)	26.1 (301)	98	124.9 ± 10.0	187.14
Ch-15-38	21	121.8 (947)	26.2 (204)	98	124.9 ± 11.4	205.38
<i>Sette-Daban zone</i>						
SM-14-01	20	130.2 (1443)	21.37 (237)	92	162.3 ± 13.8	170.66
S-15-24	16	138.4 (975)	41.6 (293)	5	89.6 ± 8.7	300.70
411	21	104.1 (1071)	30.5 (314)	54	92.4 ± 7.6	236.19

(ρ_s) Spontaneous track density of ^{238}U , (N_s) number of counted spontaneous fission tracks, (ρ_i) induced track density of ^{235}U , (N_i) number of counted induced fission tracks, ($P(\chi^2)$) chi-square probability in percent.

average age is more ancient than in samples Ch-15-51 and Ch-15-52 from the Ebeike-Khayata Ridge (Tables 2, 3). These data indicate that the studied Kyllakh samples underwent less intensive heating than the Ebeike-Khayata samples.

The samples from the 162 and 115–130 Ma age groups are characterized by a much lower dispersion and are regarded as having undergone heating above a closure temperature of the zircon track system after sedimentation of host terrigenous rocks. These ages were established in five samples: one sample from the western part of the Sette-Daban zone and four samples from the Gornostakh anticline. The obtained age range is interpreted as the time when the samples cooled below the closure temperature of the zircon track system.

Age determinations of 67–92 Ma were obtained in two samples from the Sette-Daban zone in zircon and in five samples from the Kyllakh and Sette-Daban zones in apatite. The distribution features of the track ages of individual grains in these samples indicate that the obtained determinations represent the age of cooling of samples below the closure temperature of the track systems. All grains belong to the same age population. The zircon track ages reach 90 and 92 Ma, while the apatite track ages are in the range of 67.5–86.5 Ma. The difference in ages is likely related to different closure temperatures of the track systems in apatite and zircon.

The obtained numerical modeling data based on the apatite track length distribution in three samples are evidence for two-stage cooling of the samples (Fig. 4).

The first stage corresponds to the obtained ages of 70–80 Ma for apatite and is characterized by rapid cooling from 100–120°C to about 60°C. The whole region was not subjected to thermal events until the beginning of the second stage of about 30 Ma.

The second stage, recorded in the range of 20–30 Ma, is characterized by rapid cooling from about 50–60°C to temperatures characteristic of the Earth's surface.

DISCUSSION

The obtained apatite and zircon track dates make allow conclusions on the age of uplift of the region and related deformation stages, as well as the amplitude of erosion of overthrust plates. Most samples were taken within a relatively small range of heights from 460 to 710 m above sea level (Table 1; Fig. 5); only two samples (SM-14-10 and SM-14-11) were taken at heights of 900–990 m and two samples (Ch-15-51 and 411) at heights of 140–180 m, respectively (Table 1; Fig. 1). These samples occur at a considerable distance from each other in different tectonic structures and probably for this reason, the track age is independent of the hypsometric position of the sample, in contrast to many regions of the Earth [17, 19].

Age of Deformations

In the studied structures of the western part of the South Verkhoyansk sector, the deformation track age

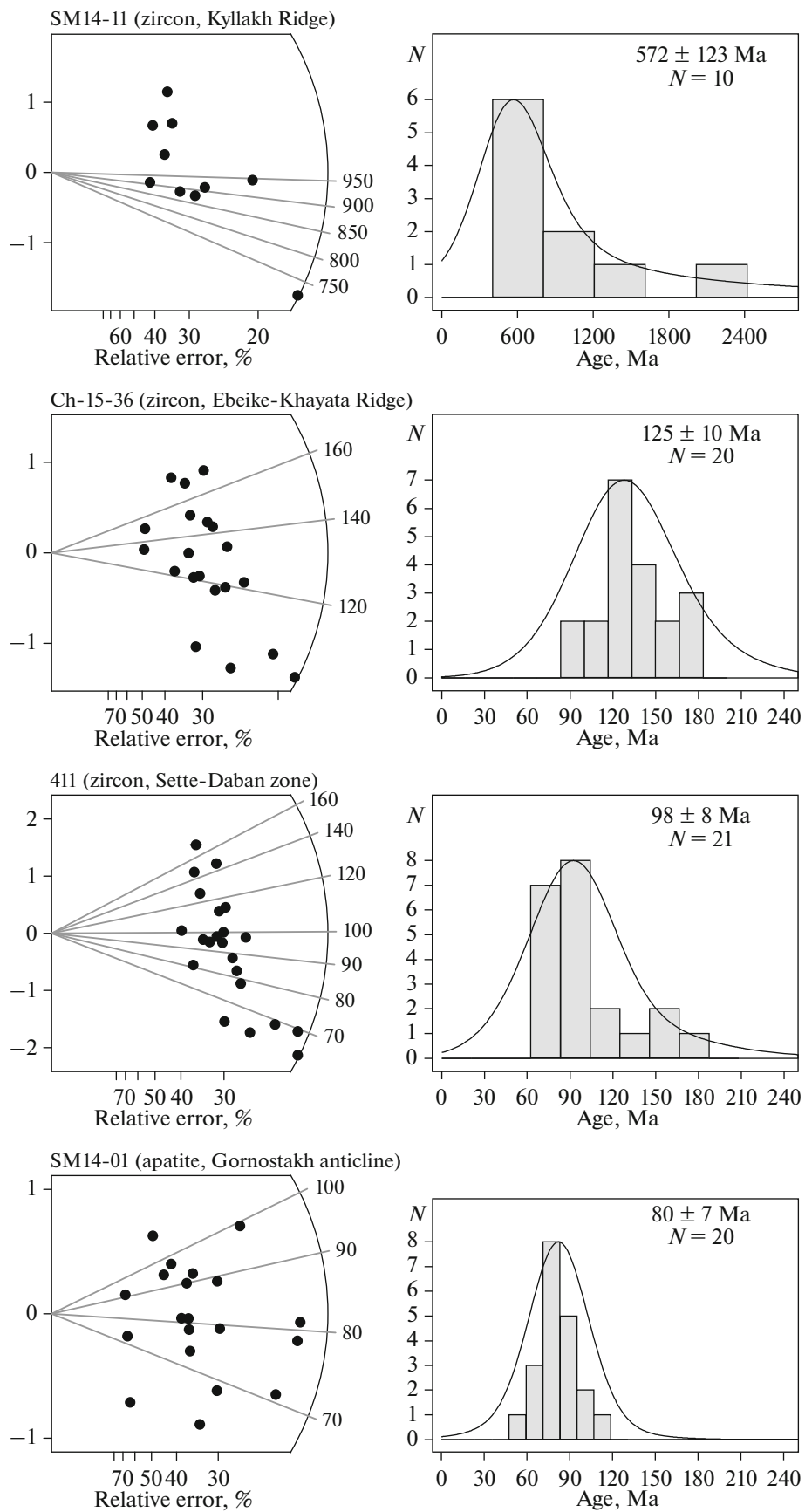


Fig. 3. Radial diagrams and histograms of age distribution for representative samples from Kyllakh Ridge (SM-14-11), Gornostakh anticline (Ch-15-36), and Sette-Daban zone (411) dated by zircon fission tracks and sample from Gornostakh anticline (SM-14-01) dated by apatite fission tracks. Radial diagrams show measurement accuracy of individual grains along *X* axis and their standard error along *Y* axis [22]. Histograms indicate peak values calculated in HeFTy software [29].

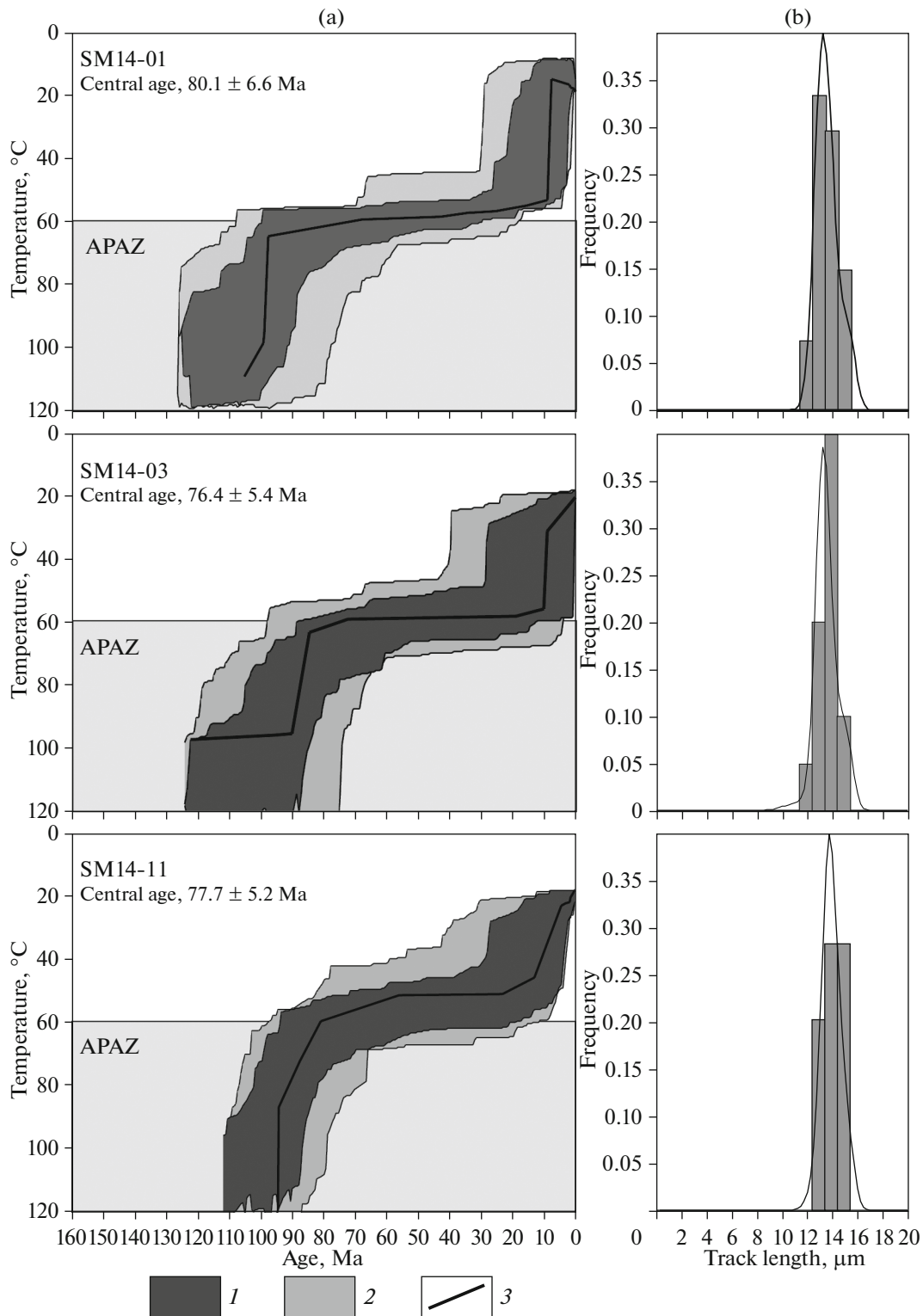


Fig. 4. Thermal modeling results obtained in HeFTy software [29]. (a) Diagram of thermal evolution from apatite fission track dating data. (APAZ) Apatite partial annealing zone. Statistical probability (according to [29]): (1) good, 50%; (2) acceptable, 5%; (3) optimal. (b) Length distribution of confined fission tracks in apatite.

can only be subdivided into three age groups (Table 4; Fig. 6):

- (1) 162 Ma,
- (2) 115–130 Ma,
- (3) 67–92 Ma.

The beginning of thrusting in this region is defined by a Vendian sandstone sample from the western part of the Sette-Daban zone (SM-14-01), which is characterized by the most ancient ZFT date of 162 ± 14 Ma. Interpretation of this age as a tectonic event is also confirmed by the $^{40}\text{Ar}/^{39}\text{Ar}$ dates of metamorphosed schists from the Sette-Daban zone [40]. The second thrusting phase occurred in the range of 115–130 Ma, which is reflected in the ZFT dates of samples from the Gornostakh anticline. ZFT ages of 90–92 Ma for the Cambrian and Ordovician samples reflect the last and, apparently, major phase of uplifting and erosion of the mountain system, which lasted to about 70 Ma, recorded by AFT ages. The apatite fission track dates are similar everywhere: from 86 to 67 Ma. This means that uplifting and erosion occurred in this age range almost simultaneously throughout the studied region. A slight westward rejuvenation of AFT ages (Table 4) is observed on the border of the Kyllakh and Sette-Daban zones, which can be explained by earlier exhumation of the interior of the fold-and-thrust belt.

According to thermal apatite modeling with track length data (Fig. 4), exhumation above the closure isotherm in apatite occurred in two stages. The first phase, corresponding to the AFT dates, is the formation of a major overthrust with subsequent erosion of mountain structures. The second phase is less pronounced in the inversion models and is limited to the age range of 20–30 Ma. Within the Kyllakh zone, there are no geological evidence for events of this age, but in the Lower Aldan depression located further north, the sequence of conglomerates with a thickness of a few hundreds of meters was deposited in the Oligocene, approximately corresponding to the age of the considered phase [4].

Amplitude of Erosion

The amplitude of erosion can be estimated by taking into account the closure temperatures for different

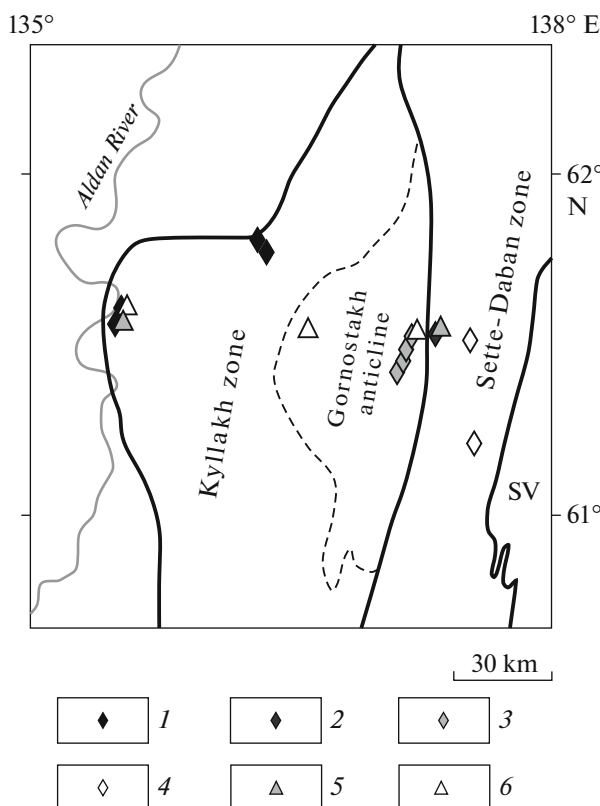


Fig. 5. Age intervals according to fission track dating data on samples from Kyllakh and Sette-Daban zones. (SV) South Verkhoyansk zone. (1–4) ZFT age intervals: (1) track system not detected; (2) 162 Ma; (3) 115–131 Ma; (4) younger than 92 Ma; (5–6) AFT age intervals: (5) 80–90 Ma; (6) 65–80 Ma.

thermal systems. With a constant heat flow and absence of large intrusions, the closure temperature of the fission track system corresponds to a certain depth. In the considered region, Mesozoic and Cenozoic intrusions are absent or they occur as sporadic basic dikes [13, 15]; they could not have considerably affected the average heat flow values. Larger granite intrusions, which could have caused variations in heat flow, are located further to the east of the Sette-Daban zone at a distance of more than 40 km from the easternmost sampling point. Taking this into account, the geothermal gradient is assumed to be max 30°C/km.

Table 4. Summary table of fission track dating data, Ma

Method	Kyllakh zone				Sette-Daban zone	
	Kyllakh Ridge	Ebeike-Khayata Ridge	Gornostakh anticline		west	east
			west	east		
AFT	86.5 77.7	No data	67.5	76.4	80.1	No data
ZFT	Not reestablished		No data	115.5 124.9 130.8	162.3	92.4 89.6

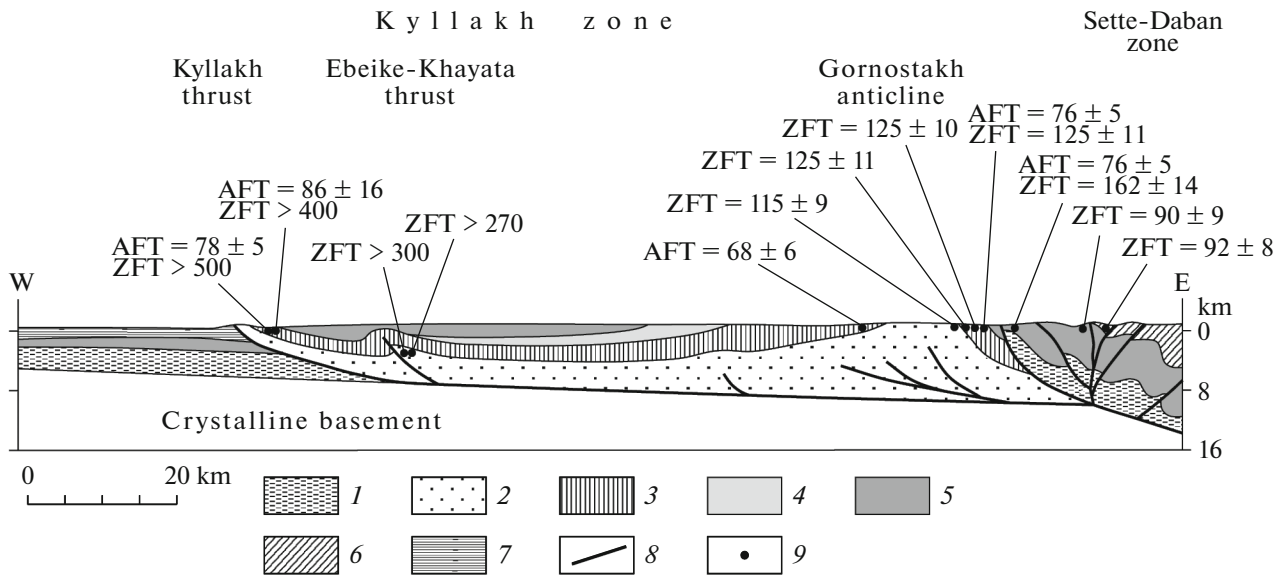


Fig. 6. Schematic section through Kyllakh and Sette-Daban zones along Belaya River with AFT and ZFT dating results, constructed using data of [10, 13, 32]. (1–4) Riphean: (1) undivided, (2) lower, (3) middle, (4) upper; (5) Vendian and Cambrian; (6) Ordovician–Devonian; (7) Jurassic; (8) faults; (9) sampling points with AFT and ZFT ages.

With this geothermal gradient, when the apatite fission track system is reset, and the zircon track system is not reset in the same sample, it means that the sample was heated to a temperature of 110–240°C and uplifted from a depth of approximately 3.5–8 km. If the zircon track system is also reset in this sample, then the upper limit is early metamorphic facies or ⁴⁰Ar/³⁹Ar mica ages. In turn, if the apatite fission track system is not reset in this sample, then it means that the sample was not heated above 110°C, and the amplitude of erosion reached max ~3.5 km.

Our paleogeographic profile shows the relationships applied to the study area (Fig. 7), indicating the location of the apatite and zircon fission track annealing zones and the ages when these zones were intersected by the corresponding samples. At present, all samples were on the Earth’s surface and, therefore, their burial depths shown in the profile characterize the amplitude of erosion. The zircon fission track system has not been reset in the frontal part of the fold-and-thrust belt. This is indicative of rock heating below the temperature of ~240 ± 30°C necessary for zircon fission track annealing. The samples taken on the Ebeike-Khayata Ridge are characterized by some rejuvenation of zircon ages, but this is no more than the samples entering the zone of partial fission track annealing. The data obtained from apatite track dating on the Kyllakh Ridge show more intensive heating than the closure temperature in apatite ~110 ± 30°C. Hence, in the frontal part of the Verkhoiansk fold-and-thrust system, vertical motion along the overthrusts, and, accordingly, the uplifting and amplitude of erosion was within ~3.5–8 km with a temperature

gradient of 30°C/km and maximum of 10 km with a gradient of 25°C/km.

Taking into account that the thickness of the Riphean–Lower Cambrian section observed in the western part of the Kyllakh zone and overlapping the studied samples is no more than 2 km, at least 1.5–2 km of sediments were located above them in the Mesozoic, which corresponds approximately to the total thickness of the Cambrian and Ordovician sections currently known only in the frontal thrust over the Ebeike-Khayata Ridge [7, 13].

Hence, the obtained AFT and ZFT dates suggest that before overthrusting and related uplifting, the Cambrian and Ordovician sequences overlay the entire western part of the Kyllakh zone and probably the southeastern part of the Siberian Platform adjacent to the frontal overthrusts.

In the eastern part of the Kyllakh zone in the Gornostakh anticline, sandstone was heated above the closure temperature in apatite and zircon. The obtained ages indicate that the Lower and Middle Riphean samples crossed the closure isotherm of the fission track system in zircon in the 115–130 Ma interval and crossed the apatite isotherm about 70 Ma. Consequently, this part of the Riphean section was buried deeper than 8 km, depending on the temperature gradient, but no more than 10–14 km, because these complexes did not undergo greenschist metamorphism. Since the thickness of the Riphean strata overlapping these samples does not exceed 3 km, they should be overlain by Vendian–Paleozoic sedimentary rocks with a thickness from 5–6 to 10–11 km and despite of the fact that the Gornostakh anticline is ascribed to the Kyllakh zone in the recent structure, a

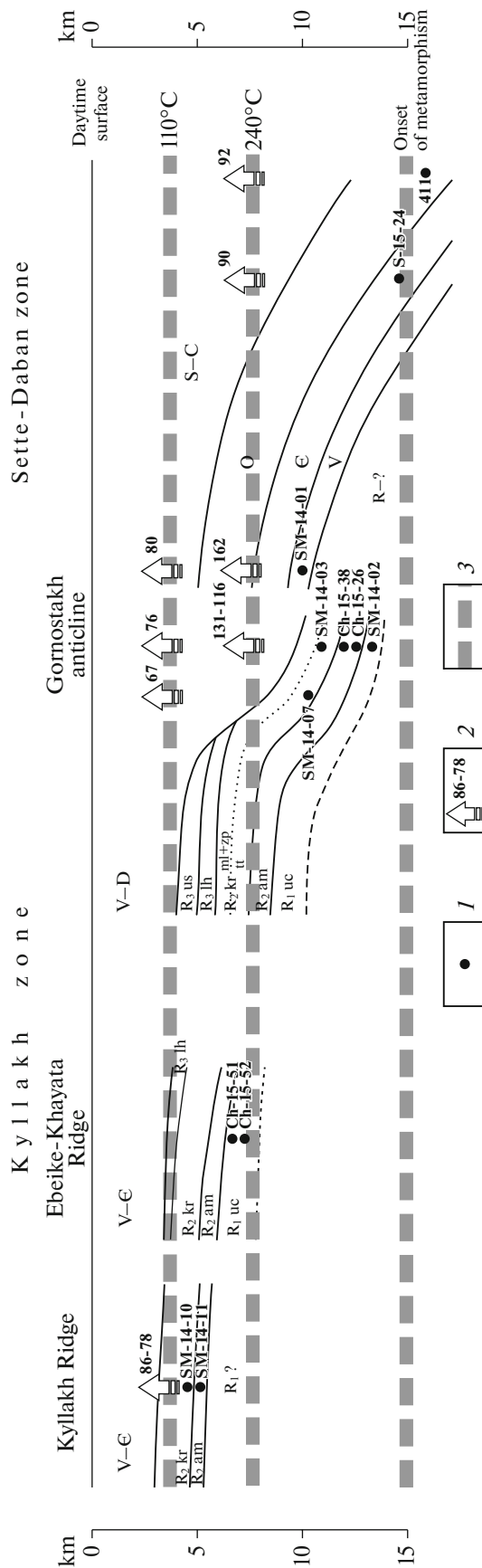


Fig. 7. Geological section reconstructed from AFT and ZFT data along Belaya River before Late Jurassic–Cretaceous deformations. Groups: (uc) Uchur (Lower Riphean); (am) Aimchan (Middle Riphean), (kr) Kerpyl (Middle Riphean); (lh) Lakhanda (Upper Riphean), (us) Ui (Upper Riphean). Kerpyl Group formations: (tt) Totta, (ml) Malga, and (zp) Tsipanda. (1) Position of samples in section; (2) time when samples crossed corresponding isotherms; (3) approximate depth of greenschist metamorphism front and isotherms of closure temperatures of fission track systems in apatite and zircon (110 and 240°C, respectively), according to [26, 39].

considerable part of it was overlapped by sediments comparable in thickness to the Paleozoic strata of the Sette-Daban zone (Fig. 2) [7, 13, 15]. Hence, the area of transition from relatively thin shelf sediments of the Siberian Palecontinent to thicker slope facies was located further west of the core of the Gornostakh anticline.

In the Sette-Daban zone, the difference in ZFT ages between samples SM-14-01 and S-15-24 (Table 1) can be interpreted as a result of variations in a thickness of the section and in the amplitude of erosion in a particular part of the sedimentary basin. A much higher thickness of the sedimentary section to the east is evidenced by the fact that more eastern samples 411 and S-15-24 crossed the closure isotherm of track system in zircon 70 Ma later than the Vendian sample SM-14-01 (Table 1). In addition, Ordovician rocks in the central part of the Sette-Daban zone, where sample 411 is taken, were subjected to initial greenschist metamorphism, indicating a deeper position of sample 411 in the sedimentary section when the uplifting and erosion processes began. Hence, the amplitude of erosion of the Paleozoic section within the Sette-Daban zone from west to east increased by a minimum of 5 km (Fig. 7).

CONCLUSIONS

The study demonstrates the potential for apatite and zircon fission track dating in reconstructing the tectonic history of overthrust systems, as well as in investigating the structure of paleobasins. The basic research results are as follows:

(1) The data on Kyllakh zircons are indicative of a systematic eastward increase in the burial depth of sedimentary complexes, which is directly related to an increase in their thickness. The thickness of the sedimentary cover and burial depth increased the most rapidly in the recent Gornostakh anticline, which can be due to location of the transition zone from the shelf of the Siberian Palecontinent to its slope.

(2) Overthrusting in the South Verkhoysansk sector began about 160 Ma ago and lasted for at least about 70 Ma. The available data are not detailed enough to establish whether the process was continuous or stepwise. The process was most likely stepwise with a

major phase at 90–70 Ma. During the major deformation phase, the age is rejuvenated from the inner (Sette-Daban) zone to the outer (Kyllakh) zone.

(3) Outcropping of sedimentary complexes and their erosion in the Oligocene are likely related to the final formation of fold-and-thrust structures in the western part of the South Verkhoyansk sector of the Verkhoyansk fold-and-thrust belt.

ACKNOWLEDGMENTS

The work was supported by a Grant of the President of the Russian Federation (MK-739.2017.5), Scientific Research Program, St. Petersburg State University (3.57.1179.2016; 3.42.979.2016).

REFERENCES

1. S. V. Malyshev, A. K. Khudolei, U. A. Glasmakher, and A. V. Shatsillo, "Results of fission track dating of detrital apatites (AFT) from sandstones of the Kyllakh zone, South Verkhoyansk region," in *Tectonics, Geodynamics, and Ore Genesis of Fold Belts and Platforms: Proceedings of the XLVIII Meeting on Tectonics* (GEOS, Moscow, 2016), Vol. 1, pp. 355–357.
2. S. V. Malyshev, A. K. Khudolei, A. V. Prokopiev, V. B. Ershova, G. G. Kazakova, and L. B. Terentyeva, "Source rocks of Carboniferous–Lower Cretaceous terrigenous sediments of the northeastern Siberian Platform: Results of Sm–Nd isotope-geochemical studies," *Russ. Geol. Geophys.* **57**, 421–433 (2016).
3. L. M. Parfenov, *Continental Margins and Island Arcs of Mesozooids in Northeast Asia* (Nauka, Novosibirsk, 1984) [in Russian].
4. L. M. Parfenov, A. V. Prokop'ev, and V. B. Spektor, "Relief of the Earth's surface and its evolution," in *Tectonics, Geodynamics, and Metallogeny of the Territory of Sakha Republic (Yakutia)*, Ed. by L. M. Parfenov and M. I. Kuz'min (MAIK Nauka/Interperiodika, Moscow, 2001), pp. 12–32.
5. V. N. Podkovyrov, L. N. Kotova, A. B. Kotov, V. P. Kovach, O. V. Graunov, and N. Yu. Zagornaya, "Provenance and source rocks of Riphean sandstones in the Uchur–Maya region (East Siberia): Implications of geochemical data and Sm–Nd isotopic systematics," *Stratigr. Geol. Correl.* **15**, 41–56 (2007).
6. A. V. Prokop'ev, *Kinematics of the Mesozoic Folding in the Western Part of South Verkhoyansk Region* (Yakutsk. Nauchn. Tsentr Sib. Otd. Akad. Nauk SSSR, Yakutsk, 1989) [in Russian].
7. A. V. Prokop'ev, L. M. Parfenov, M. D. Tomshin, and I. I. Kolodez'nikov, "Sedimentary cover of the Siberian Platform and adjacent fold-and-thrust belts," in *Tectonics, Geodynamics, and Metallogeny of the Territory of Sakha Republic (Yakutia)*, Ed. by L. M. Parfenov and M. I. Kuz'min (MAIK Nauka/Interperiodika, Moscow, 2001), pp. 113–155.
8. A. V. Prokop'ev and A. V. Deikunenko, "Deformation structures of fold-and-thrust belts," in *Tectonics, Geodynamics, and Metallogeny of the Territory of Sakha Republic (Yakutia)*, Ed. by L. M. Parfenov and M. I. Kuz'min (MAIK Nauka/Interperiodika, Moscow, 2001), pp. 156–198.
9. A. V. Prokop'ev, H. Toro, T. A. Dumitru, E. L. Miller, and D. K. Kourigan, "Formation history of thrust structures in South Verkhoyansk region (Eastern Yakutia) on the basis of fission track dating method (AFTA)," in *Evolution of Tectonic Processes in the Earth's History: Proceedings of the XXXVII Meeting on Tectonics* (Sib. Otd. Ross. Akad. Nauk, Novosibirsk, 2004), Vol. 2, pp. 86–88.
10. M. A. Semikhatov and S. N. Serebryakov, *Siberian Hypostrateotype of the Riphean* (Nauka, Moscow, 1983) [in Russian].
11. S. D. Sokolov, "Tectonics of Northeast Asia: An overview," *Geotectonics* **44**, 493–509 (2010).
12. A. V. Solov'ev, *Studies of Tectonic Processes in Convergence Zones of Lithospheric Plates: Methods of Fission Track and Structural Analysis*, Vol. 577 of *Tr. Geol. Inst. Ross. Akad. Nauk* (Nauka, Moscow, 2008) [in Russian].
13. A. I. Starnikov, N. N. Pushkar', G. A. Chernobrovkina, V. S. Grinenko, E. L. Mozalevskii, and L. N. Kovalyov, *Geological Map of Yakutia (South Verkhoyansk Block), Scale 1 : 500000* (VSEGEI, St. Petersburg, 1995).
14. A. K. Khudolei, G. A. Gur'ev, and E. A. Zubareva, "Deposits of density flows in the Sette-Daban carbonate complex, South Verkhoyansk region," *Litol. Polezn. Iskop.*, No. 5, 106–116 (1991).
15. V. A. Yan-Zhin-Shin, *Tectonics of the Sette-Daban Horst–Anticlinorium* (Yakutsk. Fil. Sib. Otd. Akad. Nauk SSSR, Yakutsk, 1983) [in Russian].
16. O. V. Yapaskurt, *Lithogenesis and Mineral Resources of Miogeosynclines* (Nedra, Moscow, 1992) [in Russian].
17. B. Andreucci, A. Castelluccio, S. Corrado, L. Jankowski, S. Mazzoli, R. Szaniawski, and M. Zattin, "Interplay between the thermal evolution of an orogenic wedge and its retro-wedge basin: An example from the Ukrainian Carpathians," *Geol. Soc. Am. Bull.* **127**, 410–427 (2015).
18. F. Bellemans, F. De Corte, and P. Van Den Haute, "Composition of SRM and CN U-doped glasses: Significance for their use as thermal neutron fluence monitors in fission track dating," *Radiat. Meas.* **24**, 153–160 (1995).
19. A. Eude, M. Roddaz, S. Bricchau, S. Brusset, Y. Calderon, P. Baby, and J. C. Soula, "Controls on timing of exhumation and deformation in the northern Peruvian eastern Andean wedge as inferred from low-temperature thermochronology and balanced cross section," *Tectonics* **34**, 715–730 (2015).
20. I. Dunkl, "Trackkey: A Windows program for calculation and graphical presentation of fission track data," *Comput. Geosci.* **28**, 3–12 (2002).
21. R. L. Fleisher, P. B. Price, and R. M. Walker, *Nuclear Tracks in Solids* (Univ. California Press, Berkeley, 1975).
22. R. F. Galbraith, "The radial plot: Graphical assessment of spread in ages," *Nucl. Tracks Radiat. Meas.* **17**, 207–214 (1990).
23. R. F. Galbraith and G. M. Laslett, "Statistical models for mixed fission track ages," *Nucl. Tracks Radiat. Meas.* **21**, 459–470 (1993).

24. J. I. Garver, "Fission-track dating," in *Encyclopedia of Paleoclimatology and Ancient Environments*, Ed. by V. Gornitz (Springer, Dordrecht, 2009), pp. 247–249.
25. A. J. W. Gleadow, "Fission track dating methods," *The 3rd School of Earth Sciences, Melbourne, Australia, 2007* (Univ. Melbourne, Melbourne, 2007), p. 74.
26. A. J. W. Gleadow and I. R. Duddy, "A natural long-term track annealing experiment for apatite," *Nucl. Tracks* **5**, 169–174 (1981).
27. A. J. W. Gleadow, I. R. Duddy, P. F. Green, and J. F. Lovering, "Confined fission track lengths in apatite: A diagnostic tool for thermal history analysis," *Contrib. Mineral. Petrol.* **94**, 405–415 (1986).
28. A. J. Hurford and P. F. Green, "The zeta age calibration of fission track dating," *Chem. Geol.* **1**, 285–317 (1983).
29. R. A. Ketchum, "Forward and inverse modeling of low-temperature thermochronometry data," *Rev. Mineral. Geochem.* **58**, 275–314 (2005).
30. A. K. Khudoley, R. H. Rainbird, R. A. Stern, A. P. Kropachev, L. M. Heaman, A. M. Zanin, V. N. Podkovyrov, V. N. Belova, and V. I. Sukhorukov, "Sedimentary evolution of the Riphean–Vendian basin of southeastern Siberia," *Precambrian Res.* **111**, 129–163 (2001).
31. A. K. Khudoley and G. A. Guriev, "Influence of syn-sedimentary faults on orogenic structure: examples from the Neoproterozoic–Mesozoic east Siberian passive margin," *Tectonophysics* **365**, 23–43 (2003).
32. A. K. Khudoley and A. V. Prokopiev, "Defining the eastern boundary of the North Asian craton from structural and subsidence history studies of the Verkhoyansk fold-and-thrust belt," in *Whence the Mountains? Inquiries into the Evolution of Orogenic Systems: A Volume in Honor of Raymond A. Price*, Vol. 433 of *Geol. Soc. Am., Spec. Pap.*, Ed. by J. W. Sears, T. A. Harms, and C. A. Evenchick (2007), pp. 391–410.
33. G. M. Laslett, W. S. Kendall, A. J. W. Gleadow, and I. R. Duddy, "Bias in measurement of fission-track length distributions," *Nucl. Tracks Radiat. Meas.* **6**, 79–85 (1982).
34. P. W. Layer, R. Newberry, K. Fujita, L. Parfenov, V. Trunilina, and A. Bakharev, "Tectonic setting of the plutonic belts of Yakutia, northeast Russia, based on $^{40}\text{Ar}/^{39}\text{Ar}$ geochronology and trace element geochemistry," *Geology* **29**, 167–170 (2001).
35. F. Lisker, B. Ventura, and U. A. Glasmacher, "Apatite thermochronology in modern geology," in *Thermochronological Methods: From Palaeotemperature Constraints to Landscape Evolution Models*, Vol. 324 of *Geol. Soc., London, Spec. Publ.*, Ed. by F. Lisker, B. Ventura, and U. A. Glasmacher (London, 2009), pp. 1–23.
36. F. W. McDowell, W. C. McIntosh, and K. A. Farley, "A precise ^{40}Ar – ^{39}Ar reference age for the Durango apatite (U–Th)/He and fission-track dating standard," *Chem. Geol.* **214**, 249–263 (2005).
37. C. W. Naeser, R. A. Zimmermann, and G. T. Cebula, "Fission-track dating of apatite and zircon: An inter-laboratory comparison," *Nucl. Tracks* **5**, 65–72 (1981).
38. L. M. Parfenov, A. V. Prokopiev, and V. V. Gaiduk, "Cretaceous frontal thrusts of the Verkhoyansk fold belt, eastern Siberia," *Tectonics* **14**, 342–358 (1995).
39. T. Tagami, R. F. Galbraith, R. Yamada, and G. M. Laslett, "Revised annealing kinetics of fission tracks in zircon and geological implications," in *Advances in Fission-Track Geochronology*, Ed. by P. Van den Haute and F. De Corte (Kluwer, Dordrecht, 1998), pp. 99–112.
40. J. Toro, A. V. Prokopiev, J. Colgan, T. Dumitru, and E. L. Miller, "Apatite fission-track thermochronology of the southern Verkhoyansk fold-and-thrust belt, Russia," *Am. Geophys. Union, Fall Meeting, 2004*, Abstr. GP44A-01. <http://adsabs.harvard.edu/abs/2004AGUFMGP44A..01T>.

Reviewers: S.D. Sokolov, E.V. Vetrov

Translated by E. Maslennikova